Published in final edited form as:
Medchemcomm. 2013 ; 4(1): 269–277. doi:10.1039/C2MD20308A.

Mechanistic insight into inhibition of two-component system signaling

Samson Francis[a], **Kaelyn E. Wilke**[a], **Douglas E. Brown**[a], and **Erin E. Carlson**[a,b]

[a]Department of Chemistry, Indiana University, 800 E. Kirkwood Avenue, Bloomington, Indiana, USA. Tel: 812-855-3665; carlsone@indiana.edu

[b]Department of Molecular and Cellular Biochemistry, Indiana University, 212 S. Hawthorne Drive, Bloomington, Indiana, USA

Abstract

Two-component signal transduction systems (TCSs) are commonly used by bacteria to couple environmental stimuli to adaptive responses. Targeting the highly conserved kinase domain in these systems represents a promising strategy for the design of a broad-spectrum antibiotic; however, development of such compounds has been marred by an incomplete understanding of the conserved binding features within the active site that could be exploited in molecule design. Consequently, a large percentage of the available TCS inhibitors demonstrate poor target specificity and act via multiple mechanisms, with aggregation of the kinase being the most notable. In order to elucidate the mode of action of some of these compounds, molecular modeling was employed to dock a suite of molecules into the ATP-binding domain of several histidine kinases. This effort revealed a key structural feature of the domain that is likely interacting with several known inhibitors and is also highly conserved. Furthermore, generation of several simplified scaffolds derived from a reported inhibitor and characterization of these compounds using activity assays, protein aggregation studies and saturation transfer differential (STD) NMR suggests that targeting of this protein feature may provide a basis for the design of ATP-competitive compounds.

Introduction

Two-component systems (TCSs) are signal transduction pathways that are ubiquitous in bacterial systems.[1, 2] Consisting of a histidine kinase (HK) and a response regulator (RR), these systems regulate diverse processes ranging from chemotaxis[3] to virulence.[4] Extracellular events activate HKs, inducing autophosphorylation of a conserved histidine (His) residue (Fig. 1). The phosphate group is subsequently transferred to an aspartate (Asp) on a cognate RR, eliciting an adaptive response such as quorum sensing,[5] antibiotic resistance,[6] or the production of virulence factors in pathogenic bacteria.[7] Furthermore, the essentiality of some of these systems in the promotion of virulence traits[8, 9] and activation of resistance mechanisms[10] makes them attractive drug targets.

To date, although ~50,000 TCS proteins have been identified from genomic sequences, most have not been characterized.[11] However, with the availability of x-ray crystal structures for a variety of HKs[12-14] and RRs,[15, 16] and recently an HK-RR complex,[17] much knowledge

†Electronic Supplementary Information (ESI) available: Supporting figures and tables are provided depicting the library of known inhibitors, additional modeling studies, kinase activity assays, protein aggregation studies, sequence alignments and experimental methods. See DOI: 10.1039/b000000x/

has been gained about the structural features that govern functionality in this family of signaling proteins. As a result, several sites have been identified for the action of chemical compounds to disrupt the intracellular signaling activities of these systems. Intervention by such a compound could occur at key junctions in the cascade (Fig. 1) including receipt of the activation signal, binding of ATP, autophosphorylation of the HK (HK~P), dephosphorylation of HK~P, phosphotransfer from HK~P to the RR, and binding of phosphorylated RR (RR~P) to the gene promoter.

The search for inhibitors capable of interrupting TCS signal transduction has yielded several classes of synthetic compounds through a combination of high-throughput screening,[18] rational design and structure-based design.[19] While these initiatives have generated large libraries of inhibitors, examples of which are shown in Fig. 2, the mechanisms of action of most of these agents remain poorly understood. For example, RWJ-49815 (**30**; Fig. 3), a representative HK inhibitor, was initially reported to exert its inhibitory activity by targeting the catalytic and ATP-binding domain (CA) of several HKs;[20] however, subsequent studies have shown that this compound inhibits HK autokinase activity non-specifically.[21] In fact, **30,** along with a large majority of compounds reported to inhibit TCS activity, do so through aggregation of the protein.[22]

Clearly, attaining specificity in the development of compounds capable of disrupting TCS signaling remains a challenging task. In recent years, there has been a heightened interest in deactivating TCS transduction by targeting the CA domain of the HK. [22,23] Similar to other classes of kinases, the catalytic core within HKs has been reported to exhibit a high degree of homology[11, 24] in both Gram-positive and Gram-negative bacteria. Exploiting such a feature could yield an inhibitor with the potential to handicap multiple TCSs in a single pathogen, perhaps providing an additional avenue towards addressing antimicrobial drug resistance. Therefore, a better understanding of the interactions that take place between the CA domain and possible ligands is paramount. Herein, we report a chemical scaffold with the potential to interact with a conserved structural feature in the CA of HKs. This scaffold was identified, optimized and validated through a combination of molecular modeling, kinase inhibition and aggregation experiments, and ligand-observed NMR studies.

Results and discussion

To examine the probable ways in which previously reported inhibitors may be interacting with an HK, we sourced a diverse set of compounds with reported activity against TCS signaling from the literature. In all, forty-five inhibitors with IC_{50} values in the range of 0.4 μM to 1000 μM were identified and added to a virtual library for screening (compounds **1-38, 41-47**; Table S1).[18, 20, 23, 25-38] This library was appended with a subset of 1000 randomly selected drug-like compounds from the ZINC small-molecule database to expand library diversity and enhance screening for actives.[39, 40] In the selection of suitable receptors from the RSCB Protein Data Bank (PDB),[41] preference was given to those that had been co-crystallized with a nucleotide and/or ligand. These included the virulence sensor PhoQ from *Salmonella typhimurium* (PDB: 3CGY)[42] and *Escherichia coli* (PDB: 1ID0),[14] the chemotaxis HK CheA (PDB: 1I58)[43] and the kinase HK853 (PDB: 2C2A),[13] both from *Thermotoga maritima*.

The combined 1045 compound set was docked into the active sites of the selected receptors using the Surflex-Dock module[44] of SYBYL[45]. The fragments-constraints feature of Surflex was implemented and utilized a portion of the co-crystallized ligand as a guide during docking (Fig. S1). In order to gauge docking accuracy, the ATP analogue AMP-PNP (**5**), was also included in the compound database. This nucleotide derivative ranked among the top 0.5% of all top-scoring compounds for one of the receptors, PhoQ (PDB: 1ID0), with the

predicted binding pose of its adenine moiety closely matching that observed crystallographically (Fig. S2). This 'positive control' helped to verify the docking and scoring parameters.

A notable aspect of many of the compounds in the inhibitor subset, particularly those in the top 10% (as surveyed across all utilized receptors), was the manner in which they interacted with a deeply buried Asp residue in the receptor active sites (Fig. S3). Hydrogen bonding interactions have been observed between a phenolic hydrogen in Radicicol and the analogous Asp in the HK PhoQ from *Salmonella typhimurium* in a co-crystallized structure.[42] We were particularly drawn to a series of high-scoring (0.1% – 7.2% across all receptors) guanidine-bearing compounds (**26**, **27**, **30**, **33;** Fig. 3A), that when docked, were predicted to interact with this active site Asp through a salt-bridge (Fig. S4). For instance, a representative docked pose of the diphenyl compound **27** reveals that a strong interaction is established between this molecule's guanidine-like head group and Asp411 within the active site of HK853 (Fig. 4). Intriguingly, compound **28** (Fig. 3A), a close derivative of **30** that lacks the guanidine moiety and instead displays an amine, did not score as well and ranked in the range of 11.5% - 35% across all four receptors. Other noteworthy interactions include a π-π stacking between the aromatic ring of **27** with Tyr384, as well as other complementary hydrophobic interactions that occur on the outskirts of the binding site.

Previous active site mapping efforts indicated that this Asp residue, which is present in the G1 box, is conserved across HKs and is involved in ATP binding.[46, 47] Using the multiple sequence alignment (MSA) of 150 HK homologs (Fig. S5)[48] rendered onto the crystal structure of HK853 from *Thermotoga maritima* (Fig. 5), we generated a map of the highly conserved residues in the ATP-binding domain. This deeply situated Asp residue, along with a pair of distal active-site residues, Asn380 and Leu446, play key roles in the binding of the nucleotide to the CA domain (Asn in N Box, Leu in G2 box; Fig. 5, inset) and may provide viable contacts for appropriately designed ATP-competitive inhibitors.

Salt-bridge mediated interactions between guanidine-like motifs and Asp residues situated in an active site have been observed before in serine proteases, thrombin,[24] and even utilized successfully as starting points for inhibitor design,[49] prompting us to further investigate this scaffold. However, the compound that was reported to be the most potent of this collection, **30**, has also been shown to elicit protein aggregation as part of its mechanism of action.[21, 22] Shoichet and co-workers reported the triphenyl-bearing compound, clotrimazole, as also being a strong protein aggregator, suggesting that large hydrophobic moieties are likely involved in this undesirable outcome.[50] Therefore, we postulated that more simplified variants of compounds **26**, **27**, **30** and **33** devoid of the rigid, hydrophobic rings would be better suited for study, with the goal of identifying a scaffold that does not cause protein aggregation (**48**, **49**; Fig. 3B).

We used our previously disclosed assay, which utilizes the fluorescent nucleotide BODIPY-FL-ATP-γS,[51] to evaluate the activity of HK853 from *Thermotoga maritima* upon subjection to the designed molecules. Inhibition of HK autophosphorylation was observed with both **48** and **49** and the commercially available HK inhibitor, NH-125 (**3**, Fig. 2; Fig. S9). The activity of compounds **48** and **49** was modest, with inhibition seen starting from 600 μM to 1 mM (Fig S6). Competition was observed between BODIPY-FL-ATP-γS and the test compounds (Fig. S7), suggesting that either the lead molecules also bind in the active site or that they aggregate the protein reversibly. When subjected to in-gel aggregation studies (Fig. S8), we confirmed that even the simplified scaffolds were still operating in a non-specific fashion by inducing aggregation of the protein, a phenomenon that was easily reversed by addition of the detergent Triton X-100. Examination of NH125 (**3**) in these assays also revealed that protein aggregates appear at concentrations where it

inhibits autophosphorylation (Fig. 6A and S8). We postulated that the aggregation potential of these compounds, all three of which contain a long alkyl tail, could be attributed to this moiety. Therefore, to further the study, we pursued the variant, **50** (Fig. 3B), that lacked the alkyl chain. Given the small size of this compound, we were unsurprised that even at concentrations nearing ~10 mM, inhibition of autophosphorylation by compound **50** was not detected in our activity assay (Fig. S10). Gel-based aggregation studies, however, using **50** confirmed that this compound did not induce aggregation of HK853 (Fig. 6B) suggesting that if this component does bind to the protein, it could provide a viable starting point for the design of an ATP-competitive inhibitor (Figs. S11 and S12). The fragment-like nature of compound **50** presented significant challenges in assessing its potential interactions with a protein receptor using standard biological assays. Therefore, we utilized a ligand-observed NMR spectroscopy technique, saturation transfer differential (STD)[52], to characterize the interactions between **50** and the receptor HK853 (Fig. 7). STD-NMR has become an invaluable tool in characterizing ligand-receptor complexes and has seen great utility in fragment-based drug discovery. Based on the nuclear-Overhauser effect, STD-NMR relies upon the selective saturation of the receptor in order to elicit resonances from any interacting ligands, distinguishing between binders and non-binders. In the presence of protein (HK853), resonances corresponding to compound **50** were observed in the STD-NMR spectrum, confirming a ligand-protein association (compare Fig. 7A and 7B). By utilizing the STD initial growth rates approach,[53] the K_d for compound **50** was determined (Fig. 8) to be 2.41 (± 0.25) mM, affording it a ligand efficiency (LE) of 0.27. If the guanidine-bearing group of **50** binds specifically in the ATP-binding site, adenosine diphosphate (ADP), the kinase reaction product, would disrupt this interaction. Thus, STD-NMR was repeated with protein and an equimolar mixture of ADP and **50**. This yielded resonances corresponding only to those of the nucleotide indicating a competitive relationship between ligand **50** and ADP (compare Fig. 7C and 7D). Additionally, mutation of the active-site Asp residue of the protein to Ala resulted in significant attenuation of ligand **50**'s affinity for HK853 as judged by the diminishment of its resonances in the STD-NMR spectrum, which demonstrated the importance of this residue in ligand binding (compare Fig. 7B and 7E). We also examined the ability of tyramine, an analogous structure that contains an amine instead of a guanidine, to interact with the histidine kinase. Extremely weak ligand signals were observed, indicating that little to no binding was taking place (compare Fig. 7F and 7G). These data are consistent with the previous finding that the guanidine-functionalized compound **30** is 10-fold more potent than the amine-containing analogue (**28**; Table S1). Collectively, our results are strongly suggestive that the simplified fragment **50** is binding in the nucleotide-binding domain of HK853 and is likely interacting with the protein via a salt-bridge with Asp411 in the active site.

With fragment **50** as a starting point, we sought to determine if a molecule with increased affinity could be designed without generation of a compound that causes protein aggregation. Our modeling studies suggest that **50** is mimicking the adenosine portion of ATP. We anticipated that appending fragment **50** with a phosphate mimic, such as a sulfonyl group, could increase compound potency. Structural data indicates that the phosphate of ADP interacts with a highly-conserved residue, N380 (Fig. 5), which could also be expected to bond to a sulfonyl moiety. Accordingly, we synthesized the modified fragment **51** (Fig. 9A) and proceeded to assess both its inhibitory and binding potentials using our activity-based assay and STD-NMR, respectively. Indeed, the evolved fragment **51** was found to not only inhibit autophosphorylation of HK853 (Fig. S13) without inducing aggregation of the protein (Fig. S14), but to also register a binding event to the receptor that is competitive with ADP (compare Fig. 9B and 9C). NMR Ranking experiments based on the STD factor values (f_{STD})[54] of ADP, tyramine, **50** and **51** (Table 1) reflected the increased affinity of **5l** for HK853 [K_d = 0.58 (± 0.06) mM]. These data also indicate as previously discerned that

binding of the guanidine-containing fragments is tighter than the related compound, tyramine, that is instead functionalized with an amine establishing the importance of this group.

Conclusions

The catalytic and ATP-binding domains of bacterial HKs represent an ideal target for the action of new antibiotics. Although challenging, the design of ATP-competitive molecules specific for this site can likely be achieved through a better understanding of its structural features. Using a combination of molecular docking and sequence alignments, we have identified that the conserved Asp residue in the active site of HKs may interact with a portion of the compounds reported to have TCS inhibitory activities. Also, by deconstructing a series of known aggregators, we have identified a fragment (**50**) that likely binds with this residue, providing a basis for the design of selective HK inhibitors. Elaboration of this fragment into the sulfonyl **51**, which may interact similarly to AMP, resulted in the identification of a compound with increased affinity. Our studies suggest that rational design is a viable avenue for the generation of potent inhibitors that specifically preclude autophosphorylation in this family of proteins.

Experimental section

Synthetic methods

General information—All materials and chemicals were purchased from EMD Chemicals, Sigma, Aldrich, J.T. Baker, (unless noted otherwise) and were used without further purification. Solvents were purchased as anhydrous and not further purified. ^{1}H nuclear magnetic resonance (NMR) spectra were recorded on a Varian I500 or a Varian VXR-400 instrument. Chemical shifts are reported relative to residual solvent peaks in parts per million. Apparent first-order multiplicities are indicated by s, singlet; d, doublet; dd, doublet of doublets; t, triplet; dt, doublet of triplets; q, quartet; m, multiplet. Analytical TLC was performed on Silica Gel 60 F_{254} plates, E. Merck by detection with 254 nm UV light and then spray-heat development using a *p*-anisaldehyde-sulfuric acid reagent. Column chromatography was run by using silica gel (63-200 mesh).

1-(4-heptyloxy)phenethyl)guanidine (48): Compound **52** (0.011 g, 0.029 mmol) was added to a round-bottom flask equipped with a teflon coated magnetic stir bar containing 15 mL of acetone. Potassium carbonate (0.040 g, 0.29 mmol) was added to the flask and the reaction mixture stirred at reflux for 1 h. 1-bromoheptane (6.2 mg, 0.035 mmol) was added, followed by NaI (2.2 mg, 0.014 mmol) and the mixture stirred overnight at reflux. The mixture was cooled to room temperature and the solvent removed *in vacuo*. The crude material was re-dissolved in 30 mL dichloromethane (DCM) and an equal part water and extracted 3 times with DCM. The organic layers were pooled, dried over $MgSO_4$ and the solvent evaporated *in vacuo*. The crude product was further purified via column chromatography (2:0.6 Hexanes:EtOAc) to afford the Boc-protected derivative of **48** (9.7 mg, 0.020 mmol, 70% yield) which then underwent a 2 h deprotection step in a stirred solution of 1 mL dichloromethane and 1 mL TFA. Evaporation of the solvents *in vacuo* followed by chromatography through a plug of neutral alumina (0.1:2 MeOH:$CHCl_3$) afforded **48** (5.1 mg, 0.018 mmol, 91 % yield) ^{1}H NMR (400 MHz, CD_3OD) δ 7.16 (d, *J* = 8.3 Hz, 2H), 6.87 (d, *J* = 8.3 Hz, 2H), 3.94 (t, *J* = 6.4 Hz, 2H), 3.41 (t, *J* = 7.0 Hz, 2H), 2.81 (t, *J* = 6.9 Hz, 2H), 1.82 – 1.71 (m, 2H), 1.51 – 1.43 (m, 2H), 1.41 – 1.32 (m, 6H), 0.91 (t, *J* = 6.1 Hz, 3H). ^{13}C NMR δ, 15.0, 24.3, 27.8, 30.8, 31.1, 33.6, 35.8, 44.5, 69.7, 116.4, 131.4, 160.2 MS (m/z): $[M+H]^+$ calcd for $C_{16}H_{27}N_3O$ 278.2232; found 278.2220.

1-(4-(decyloxy)phenethyl)guanidine (49): Preparation of compound **49** used a method similar to that of **48** (5.1 mg, 0.016 mmol, 85 % yield) ^{1}H NMR (400 MHz, CD_3OD) δ 7.16 (d, *J* = 7.9 Hz, 2H), 6.88 (d, *J* = 8.5 Hz, 2H), 3.95 (t, *J* = 6.5 Hz, 2H), 3.42 (t, *J* = 7.0 Hz, 2H), 2.82 (t, *J* = 7.0 Hz, 2H), 1.79 – 1.73 (m, 2H), 1.51 – 1.45 (m, 2H), 1.32 (s, 12H), 0.92 (t, *J* = 6.4 Hz, 3H). ^{13}C NMR δ 14.4, 23.7, 27.2, 30.43, 30.44, 30.5, 30.68, 30.73, 33.1 35.1 43.9 69.0, 115.8, 130.8, 159.55 MS (m/z): $[M+H]^+$ calcd for $C_{19}H_{34}N_3O$ 320.2702; found 320.2715.

1-(4-hydroxyphenethyl)guanidine (50): To a 25 mL round-bottomed flask charged with a magnetic stir bar and under a nitrogen atmosphere was added 4-(2-aminoethyl)phenol (0.10 g, 0.73 mmol) and triethylamine (0.10 ml, 0.73 mmol) to 10 mL of dichloromethane. After stirring for 10 min., 1,3-di-boc-2-(trifluoromethylsulfonyl)guanidine (0.31 g, 0.80 mmol) was added and allowed to stir for an additional 4 h. TLC confirmed the formation of product and the solvents were removed *in vacuo* to yield a light brown crude oil, which was purified via column chromatography (2:1 Hexanes:EtOAc) to afford **52**, the protected variant of **50** (0.22 g, 0.58 mmol, 79% yield). ^{1}H NMR (400 MHz, CD_2Cl_2) δ 7.00 (d, *J* = 8.4 Hz, 2H), 6.75 (d, *J* = 8.5 Hz, 2H), 3.53 (t, *J* = 7.1 Hz, 2H), 2.75 (t, *J* = 7.3 Hz, 2H), 1.48 (s, 9H), 1.43 (s, 9H). Compound **52** (0.10 g, 0.26 mmol) was taken up in 1 mL dichloromethane and 1 mL trifluoroacetic acid and the reaction mixture was stirred for 2 h at r.t. after which the solvents were removed *in vacuo*. Purification of the crude material was accomplished by passage through a plug of neutral alumina (0.1:2 MeOH:$CHCl_3$) to afford compound **51** (0.046g, 0.256 mmol, 97 % yield). ^{1}H NMR (400 MHz, CD_3OD) δ 7.04 (d, *J* = 8.1 Hz, 2H), 6.71 (d, *J* = 8.1 Hz, 2H), 3.36 (t, *J* = 7.0 Hz, 2H), 2.75 (t, *J* = 7.0 Hz, 2H). ^{13}C NMR δ 33.7, 42.5, 115.0, 129.4, 155.9 MS (m/z): $[M+H]^+$ calcd for $C_9H_{14}N_3O$ 180.1137; found 180.1133.

1-(4-methylsulfonyl)phenethyl)guanidine (51): Preparation of compound **51** used a method similar to that of **50**. ^{1}H NMR (400 MHz, CD_3OD) δ 7.93 (d, *J* = 8.1 Hz, 2H), 7.56 (d, *J* = 8.0 Hz, 2H), 3.53 (t, *J* = 6.9 Hz, 2H), 3.12 (s, 3H), 3.02 (t, *J* = 7.0 Hz, 2H). ^{13}C NMR δ 34.3, 41.5, 43.7, 127.1, 129.9, 139.1, 144.7, 156.9 MS (m/z): $[M+H]^+$ calcd for $C_{10}H_{15}N_3O_2S$ 242.0963 found 242.0965

Biochemical methods

General methods and information—Reagents were obtained from J.T. Baker, Mallinkrodt, Sigma, IBI, VWR, EMD Biosciences, Bio-Rad and Fisher. BODIPY-FL-ATPγS was purchased from Invitrogen, NH125 from Tocris Bioscience, and BS^3-d_0 from Thermo Scientific.

Gel electrophoresis: For sodium dodecyl sulfate-polyacrylamide gel electrophoresis (SDS-PAGE), tris-glycine gels were used. The stacking gel was 4.5% acrylamide, and the resolving gel was 10% acrylamide. For native-PAGE, tris-glycine gels were prepared with 7.5% acrylamide. Electrophoresis parameters were 180 V, 400 mA, and 60 W for 1 h.

In-gel fluorescence detection: After SDS-PAGE, gels were washed 3 times with water and scanned on a Typhoon Variable Mode Imager 9210 (Amersham Biosciences) using 526-nm (short-pass filter) detection for BODIPY (λ_{ex}: 504 nm, λ_{em}: 514 nm). Imaging of gels and/or integration of fluorescence bands were performed in ImageJ.

Silver staining: All steps were carried out at RT with an orbital shaker to ensure agitation, and solutions were discarded after each step. After SDS- or native-PAGE, gels were fixed for 1 h in 20% ethanol, 1% acetic acid. Gels were then washed in 20% ethanol for 10 min. After pre-treating the gel for 1 min in 0.02% sodium thiosulfate, gels were washed for 1 min

in water. Gels were incubated with 0.1% silver nitrate for 20 min and again rinsed for 1 min in water. Developing solution (2% sodium carbonate, 20 μL 37% formaldehyde) was incubated with gels for approximately 10 min, or until protein bands were visible, and development was halted with 5% acetic acid for 10 min. Gels were then submerged in water.

Buffers: The reaction buffer used in activity assays with BODIPY-FL-ATPγS was 50 mM Tris-HCl, 0.2 M KCl, 5 mM $MgCl_2$, final pH 7.8. The 2X SDS-PAGE sample loading buffer contained 125 mM Tris, pH 6.8, 20% glycerol (v/v), 4% SDS (w/v), 5% BME (v/v), and 0.2% bromophenol blue (w/v). Native-PAGE sample loading buffer contained 40 mM Tris, pH 7.5, 8% glycerol (v/v), and 0.08% bromophenol blue (w/v). The electrophoresis running buffer for SDS-PAGE was diluted 10-fold from Novex Tris-Glycine SDS Running buffer (10X; Invitrogen). Native-PAGE electrophoresis buffer contained 83 mM Tris, pH 9.4, and 33 mM glycine.

Assessment of autophosphorylation (competitive ABPP): All analogues were dissolved in DMSO, and the final concentration of DMSO in each sample was kept at or below 5% (v/v). These concentrations of DMSO were found to have no effect on the activity labeling. Purified HK853 (600 ng) in reaction buffer was incubated with varied concentrations of analogues for 30 min. Labeling was achieved by adding 1 μL BODIPY-FL-ATPγS (B-ATPγS; 2 μM final concentration) to each sample. Individual mixtures were incubated at RT for 1 h in the dark to prevent fluorophore photobleaching. After incubation, reactions were quenched with 2X SDS-PAGE loading buffer before running on SDS-PAGE gels (samples were not heated). After analyzing gels by fluorescence, they were coomassie stained.

Aggregation analysis of NH125 (3), 48, 49, 50 and 51 (native-PAGE): Purified HK853 (0.44 μM) was prepared in 20 mM HEPES, pH 7.5. Samples of 20 μL HK853 were mixed with 1 μL 2.18% Triton X-100 in HEPES (0.1% final Triton X-100) or HEPES alone. Various concentrations of analogues were added, and reactions were incubated at RT for 4 h. DMSO concentrations were no greater than 5% (v/v). Native-PAGE sample loading buffer was added prior to loading on the gels. Silver staining was used for protein visualization.

Aggregation analysis of NH125 (3), 48, 49, 50 and 51 (SDS-PAGE): Purified HK853 (0.44 μM) was prepared in 20 mM HEPES, pH 7.5. Samples of 20 μL HK853 were mixed with 1 μL 2.18% Triton X-100 in HEPES (0.1% final Triton X-100) or HEPES alone. Various concentrations of analogues were added, and reactions were incubated at RT for 4 h. The crosslinker bis(sulfosuccinimidyl)suberate (BS^3-d_0) was suspended in DMSO and was added at a 100-fold molar excess over the protein. Total DMSO concentrations were no greater than 5% (v/v). Crosslinking reactions were incubated another 2 h at RT and quenched with a final concentration of 20 mM ammonium bicarbonate to bring individual samples to 25 μL. SDS-PAGE sample loading buffer was added prior to loading on the gels. Silver staining was used to visualize proteins.

Computational methods

General information—All molecular modeling operations were performed using SYBYL X 2.0 on a quad-core Intel Core i3 workstation operating at 3.06 GHz equipped with 4 GB 1333MHz DDR 3 RAM. Visualization of docked poses was accomplished using the latest available release of UCSF Chimera.

Target selection: Four protein targets were retrieved from the RSCB Protein Data Bank using the following accession codes: 3CGY (virulence sensor PhoQ, *Salmonella*

typhimurium) and 1ID0 (virulence sensor, *Escherichia coli*), 1I58 (chemotaxis HK CheA, *Thermotoga maritima*) and 2C2A (the kinase HK 853, *Thermotoga maritima*). The receptors were processed in order to remove co-crystallized ligands and water molecules followed by the addition of hydrogens using the Prepare Protein Structure tool in SYBYL. Atom types were assigned using the AMBER method and a staged-minimization was performed on the hydrogens in the biopolymer using the AMBER7 FF99 force field.

Compound library: Compounds with reported activity against TCS transduction were constructed using the SYBYL sketcher, and their conformations were arrived at by optimization via minimization with the Tripos force field. Electrostatic charges were then assigned using the Gasteiger-Hückel method. A larger set of 1000 drug-like compounds was obtained from the ZINC small-molecule database and appended to the database. The combined set was prepared for docking using the “Sanitize” protocol in the Ligand Structure Preparation tool found in SYBYL, which removed all counter ions.

Docking of compounds: The active sites of all receptors were defined based on the coordinates of the co-crystallized ligand and the Protomol Generation Mode in Surflex using default settings. A portion of the co-crystallized ligand was retained and used as a guide for the placement of compounds into the active site during docking.

Scoring: Upon completion of the docking screens, the CScore module in SYBYL was used to rank the poses of docked ligands. Although the primary criterion for inspecting high-scoring members was the Surflex assigned score, these highly-ranked compounds were also visually inspected for favorable interactions with pertinent active-site residues. Compounds that appeared to make interactions in the region leading into the active site or had overly hydrophobic contacts with the binding pocket were de-prioritized for further consideration.

Supplementary Material

Refer to Web version on PubMed Central for supplementary material.

Acknowledgments

We thank D. Ma for assistance with the NMR spectrometers, C. Dann and T. Stone for helpful discussions and F. Hardin, Jr. for generating HK853 protein. This work was supported by NIH R00GM82983, NIH DP2OD008592, a Pew Biomedical Scholar Award (E.E.C.), and an Indiana University Quantitative and Chemical Biology Training Fellowship (K.E.W.).

references

1. Stock AM, Robinson VL, Goudreau PN. Annu. Rev. Biochem. 2000; 69:183–215. [PubMed: 10966457]
2. Egger LA, Park H, Inouye M. Genes Cells. 1997; 2:167–184. [PubMed: 9189755]
3. Stock A, Chen T, Welsh D, Stock J. Proc. Natl. Acad. Sci. U. S. A. 1988; 85:1403–1407. [PubMed: 3278311]
4. Clough SJ, Lee KE, Schell MA, Denny TP. J. Bacteriol. 1997; 179:3639–3648. [PubMed: 9171411]
5. Antunes LCM, Ferreira RBR, Buckner MMC, Finlay BB. Microbiology. 2010; 156:2271–2282. [PubMed: 20488878]
6. Guenzi E, Gasc A-M, Sicard MA, Hakenbeck R. Mol. Microbiol. 1994; 12:505–515. [PubMed: 8065267]
7. Paterson GK, Blue CE, Mitchell TJ. J. Med. Microbiol. 2006; 55:355–363. [PubMed: 16533981]
8. Beier D, Gross R. Curr. Opin. Microbiol. 2006; 9:143–152. [PubMed: 16481212]

9. Reading NC, Rasko DA, Torres AG, Sperandio V. Proc. Natl. Acad. Sci. U. S. A. 2009; 106:5889–5894. [PubMed: 19289831]
10. Cangelosi GA, Do JS, Freeman R, Bennett JG, Semret M, Behr MA. Antimicrob. Agents Chemother. 2006; 50:461–468. [PubMed: 16436697]
11. Gao R, Stock AM. Annu. Rev. Microbiol. 2009; 63:133–154. [PubMed: 19575571]
12. Bick MJ, Lamour V, Rajashankar KR, Gordiyenko Y, Robinson CV, Darst SA. J. Mol. Biol. 2009; 386:163–177. [PubMed: 19101565]
13. Marina A, Waldburger CD, Hendrickson WA. EMBO J. 2005; 24:4247–4259. [PubMed: 16319927]
14. Marina A, Mott C, Auyzenberg A, Hendrickson WA, Waldburger CD. J. Biol. Chem. 2001; 276:41182–41190. [PubMed: 11493605]
15. Park AK, Moon JH, Lee KS, Chi YM. Biochem. Biophys. Res. Commun. 2012; 421:403–407. [PubMed: 22521891]
16. Yamada S, Sugimoto H, Kobayashi M, Ohno A, Nakamura H, Shiro Y. Structure (London, England: 1993). 2009; 17:1333–1344.
17. Casino P, Rubio V, Marina A. Cell. 2009; 139:325–336. [PubMed: 19800110]
18. Qin Z, Zhang J, Xu B, Chen L, Wu Y, Yang X, Shen X, Molin S, Danchin A, Jiang H, Qu D. BMC Microbiol. 2006; 6:96. [PubMed: 17094812]
19. Tang YT, Gao R, Havranek JJ, Groisman EA, Stock AM, Marshall GR. Chem. Biol. Drug Des. 2012; 79:1007–1017. [PubMed: 22339993]
20. Barrett JF, Goldschmidt RM, Lawrence LE, Foleno B, Chen R, Demers JP, Johnson S, Kanojia R, Fernandez J, Bernstein J, Licata L, Donetz A, Huang S, Hlasta DJ, Macielag MJ, Ohemeng K, Frechette R, Frosco MB, Klaubert DH, Whiteley JM, Wang L, Hoch JA. Proc. Natl. Acad. Sci. U. S. A. 1998; 95:5317–5322. [PubMed: 9560273]
21. Theodorou EC, Theodorou MC, Kyriakidis DA. Cell. Signal. 2011; 23:1327–1337. [PubMed: 21443947]
22. Stephenson K, Yamaguchi Y, Hoch JA. J. Biol. Chem. 2000; 275:38900–38904. [PubMed: 10978341]
23. Gilmour R, Foster JE, Sheng Q, McClain JR, Riley A, Sun P-M, Ng W-L, Yan D, Nicas TI, Henry K, Winkler ME. J. Bacteriol. 2005; 187:8196–8200. [PubMed: 16291694]
24. Škedelj V, Tomašić T, Mašič LP, Zega A. J. Med. Chem. 2011; 54:915–929. [PubMed: 21235241]
25. Foster JE, Sheng Q, McClain JR, Bures M, Nicas TI, Henry K, Winkler ME, Gilmour R. Microbiology. 2004; 150:885–896. [PubMed: 15073298]
26. Furuta E, Yamamoto K, Tatebe D, Watabe K, Kitayama T, Utsumi R. FEBS Lett. 2005; 579:2065–2070. [PubMed: 15811319]
27. Hilliard JJ, Goldschmidt RM, Licata L, Baum EZ, Bush K. Antimicrob. Agents Chemother. 1999; 43:1693–1699. [PubMed: 10390224]
28. Hlasta DJ, Demers JP, Foleno BD, Fraga-Spano SA, Guan J, Hilliard JJ, Macielag MJ, Ohemeng KA, Sheppard CM, Sui Z, Webb GC, Weidner-Wells MA, Werblood H, Barrett JF. Bioorg. Med. Chem. Lett. 1998; 8:1923–1928. [PubMed: 9873460]
29. Kanojia RM, Murray W, Bernstein J, Fernandez J, Foleno BD, Krause H, Lawrence L, Webb G, Barrett JF. Bioorg. Med. Chem. Lett. 1999; 9:2947–2952. [PubMed: 10571153]
30. Kitayama T, Iwabuchi R, Minagawa S, Sawada S, Okumura R, Hoshino K, Cappiello J, Utsumi R. Bioorg. Med. Chem. Lett. 2007; 17:1098–1101. [PubMed: 17157007]
31. Li N, Wang F, Niu S, Cao J, Wu K, Li Y, Yin N, Zhang X, Zhu W, Yin Y. BMC Microbiol. 2009; 9:129. [PubMed: 19558698]
32. Okada A, Gotoh Y, Watanabe T, Furuta E, Yamamoto K, Utsumi R. Methods Enzymol. 2007; 422:386–395. [PubMed: 17628150]
33. Qin Z, Lee B, Yang L, Zhang J, Yang X, Qu D, Jiang H, Molin S. FEMS Microbiol. Lett. 2007; 273:149–156. [PubMed: 17578527]
34. Ramström H, Bourotte M, Philippe C, Schmitt M, Haiech J, Bourguignon J-J. J. Med. Chem. 2004; 47:2264–2275. [PubMed: 15084125]

35. Roychoudhury S, Blondelle SE, Collins SM, Davis MC, McKeever HD, Houghten RA, Parker CN. Mol. Diversity. 1998; 4:173–182.
36. Roychoudhury S, Zielinski NA, Ninfa AJ, Allen NE, Jungheim LN, Nicas TI, Chakrabarty AM. Proc. Natl. Acad. Sci. U. S. A. 1993; 90:965–969. [PubMed: 8381538]
37. Sui Z, Guan J, Hlasta DJ, Macielag MJ, Foleno BD, Goldschmidt RM, Loeloff MJ, Webb GC, Barrett JF. Bioorg. Med. Chem. Lett. 1998; 8:1929–1934. [PubMed: 9873461]
38. Trew SJ, Wrigley SK, Pairet L, Sohal J, Shanu-Wilson P, Hayes MA, Martin SM, Manohar RN, Chicarelli-Robinson MI, Kau DA, Byrne CV, Wellington EM, Moloney JM, Howard J, Hupe D, Olson ER. J. Antibiot. (Tokyo). 2000; 53:1–11. [PubMed: 10724001]
39. Pham TA, Jain AN. J. Med. Chem. 2005; 49:5856–5868. [PubMed: 17004701]
40. Irwin JJ, Shoichet BK. J. Chem. Inf. Model. 2004; 45:177–182. [PubMed: 15667143]
41. RSCB Protein Data Bank. http://www.pdb.org
42. Guarnieri MT, Zhang L, Shen J, Zhao R. J. Mol. Biol. 2008; 379:82–93. [PubMed: 18440021]
43. Bilwes AM, Quezada CM, Croal LR, Crane BR, Simon MI. Nat. Struct. Biol. 2001; 8:353–360. [PubMed: 11276258]
44. Jain A. J. Comput.-Aided Mol. Des. 2007; 21:281–306. [PubMed: 17387436]
45. Associates, T. Certara, St.; Louis, MI: 2012.
46. Hirschman A, Boukhvalova M, VanBruggen R, Wolfe AJ, Stewart RC. Biochemistry. 2001; 40:13876–13887. [PubMed: 11705377]
47. Bilwes AM, Quezada CM, Croal LR, Crane BR, Simon MI. Nat. Struct. Mol. Biol. 2001; 8:353–360.
48. Ashkenazy H, Erez E, Martz E, Pupko T, Ben-Tal N. Nucleic Acids Res. 2010; 38:W529–W533. [PubMed: 20478830]
49. Olsen JA, Banner DW, Seiler P, Obst Sander U, D'Arcy A, Stihle M, Müller K, Diederich F. Angew. Chem., Int. Ed. 2003; 42:2507–2511.
50. Seidler J, McGovern SL, Doman TN, Shoichet BK. J. Med. Chem. 2003; 46:4477–4486. [PubMed: 14521410]
51. Wilke KE, Francis S, Carlson EE. J. Am. Chem. Soc. 2012; 134:9150–9153. [PubMed: 22606938]
52. Mayer M, Meyer B. J. Am. Chem. Soc. 2001; 123:6108–6117. [PubMed: 11414845]
53. Angulo J, Enríquez-Navas PM, Nieto PM. Chemistry – A European Journal. 2010; 16:7803–7812.
54. Barelier S, Pons J, Gehring K, Lancelin J-M, Krimm I. J. Med. Chem. 2010; 53:5256–5266. [PubMed: 20575554]

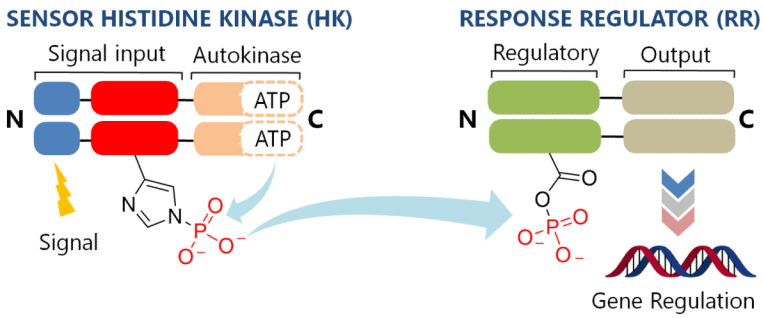

Fig. 1.

The two-component system signaling (TCS) cascade. Upon detection of an appropriate signal, autophosphorylation occurs at a conserved His residue of the HK, followed by phosphoryl group transfer to an Asp residue of the RR. A typical function for the RR is gene regulation.

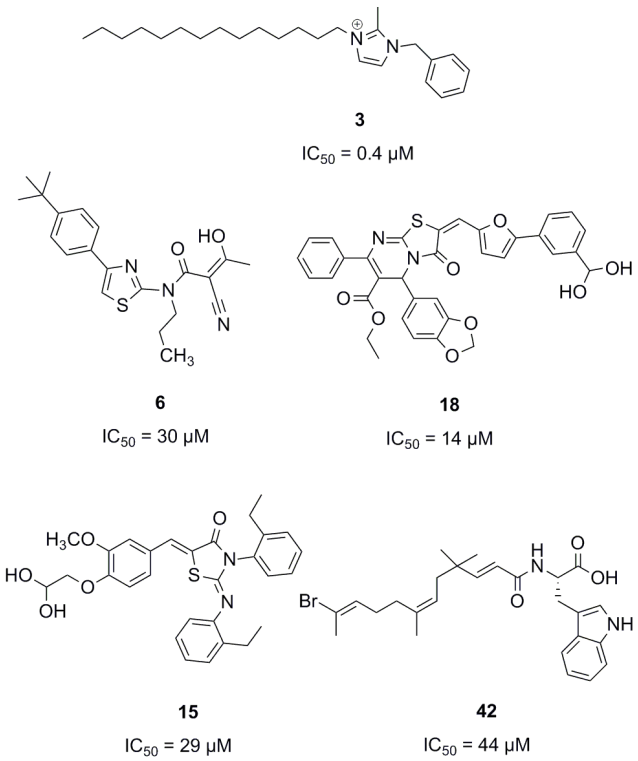

Fig. 2.
Molecules reported to inhibit TCS activity.

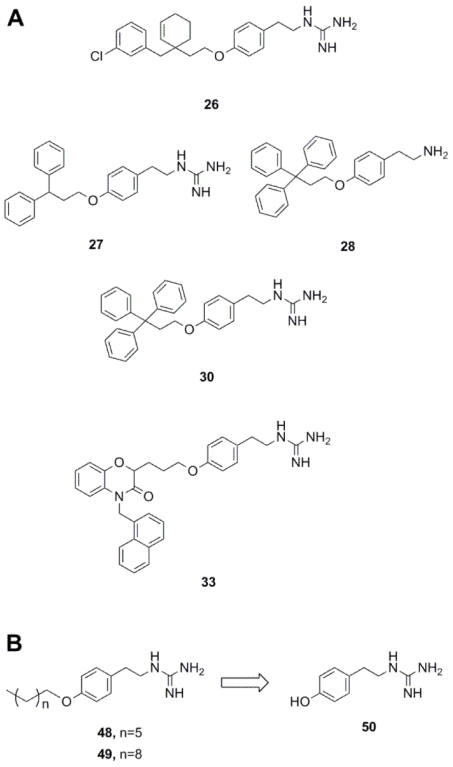

Fig. 3.

Compounds bearing guanidine moieties. (A) Subset of compounds predicted to interact with an active site Asp using molecular modeling. (B) Simplified variants of compounds **26**, **27**, **30** and **33**. Further deconstruction of these compounds resulted in the fragment-like compound **50.**

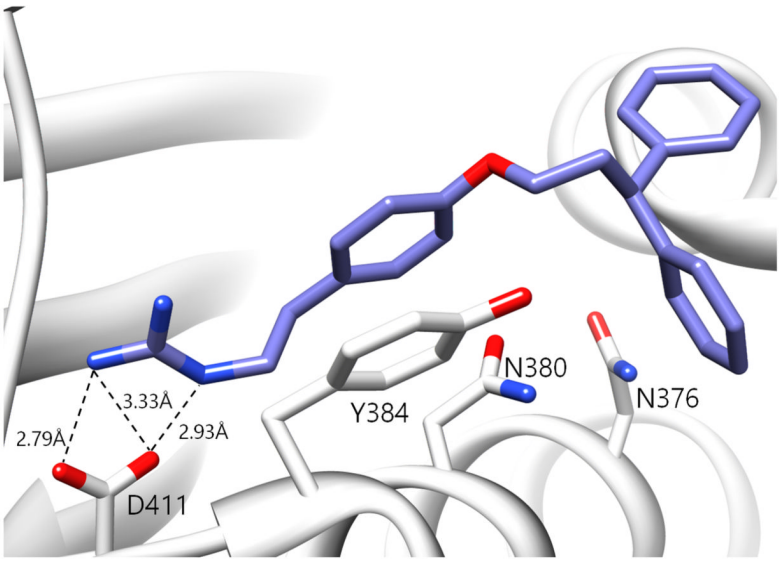

Fig. 4.

Predicted binding pose of compound **27** in the active site of HK853. The guanidine moiety of **27** forms a salt-bridge with D411. The ligand is also projected to participate in **π-π** stacking interactions with Y384.

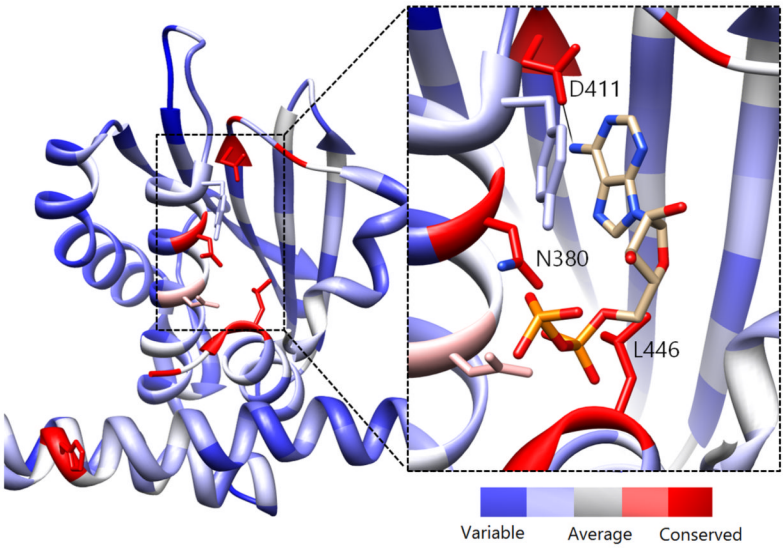

Fig. 5.

Evolutionary profile of active site residues in HKs. Derived from the sequence alignment of 150 HK homologs and rendered onto HK853 from *Thermotoga maritima*. Red colored residues/areas indicate high degrees of evolutionary conservation while blue regions indicate variations in conservation. Inset: Co-crystallized structure of ADP in the CA domain of HK853[13] illustrating residues that are involved in binding of the nucleotide. The measured distance between the exocylic N of ADP and D411 is 2.83 Å.

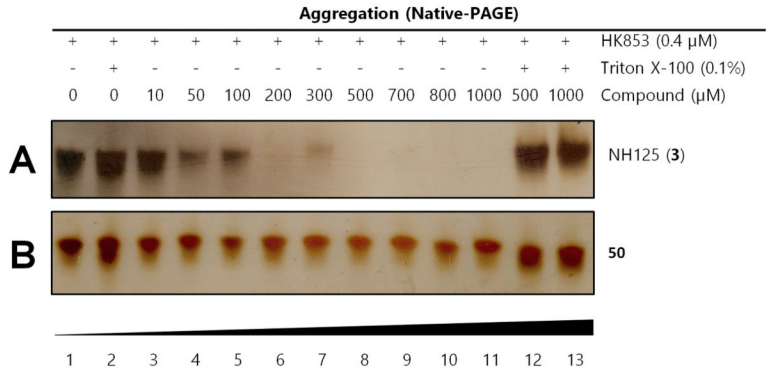

Fig. 6.

Gel-based aggregation studies using native-PAGE. (A) NH125 (**3**) induces aggregation of the protein starting at concentrations as low as 50 μM as evidenced by the disappearance of protein bands (B) Compound **50** does not aggregate HK853 even at concentrations as high as 1 mM.

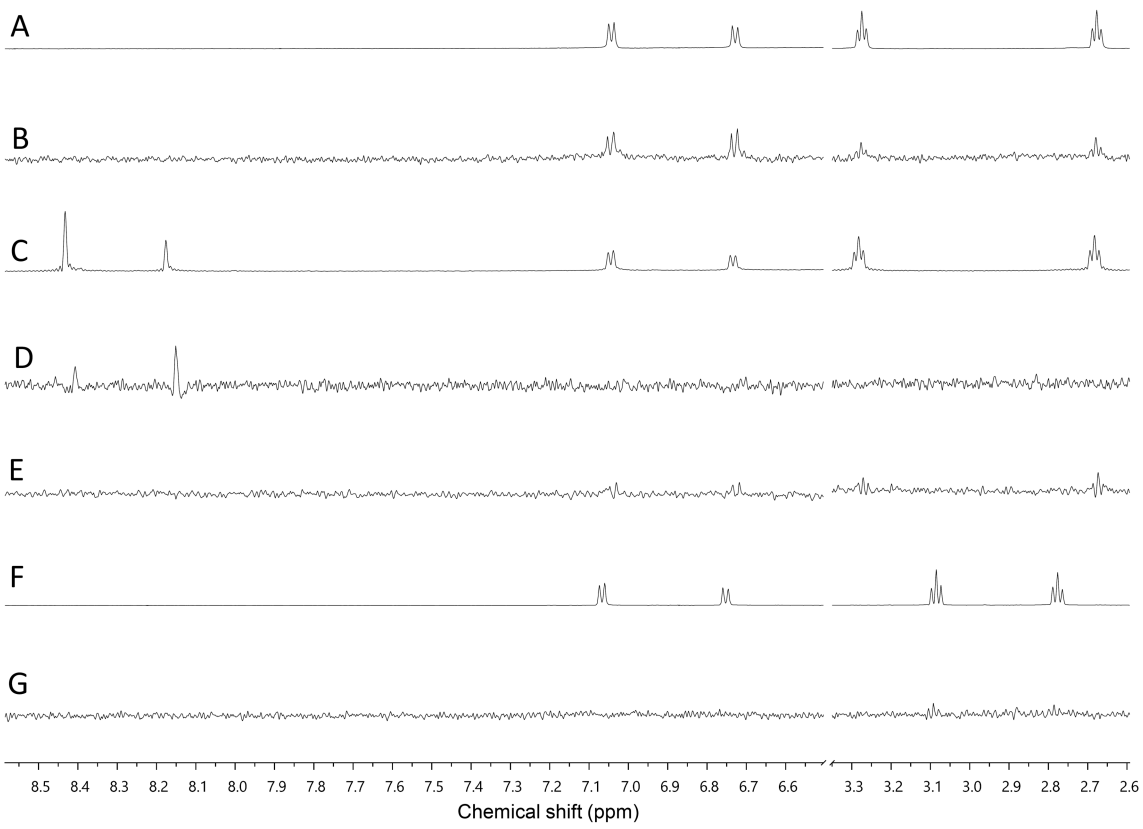

Fig. 7.

Assessment of binding using saturation transfer differential (STD) experiments (A) ^{1}H spectrum of **50** and HK853 (B) ^{1}H STD-NMR spectrum of **50** and HK853 (C) ^{1}H NMR spectrum of **50**, ADP and HK853 (D) ^{1}H STD-NMR spectrum of **50**, ADP and HK853 (E) ^{1}H STD-NMR spectrum of **50** and mutated (D411A) HK853 (F) ^{1}H spectrum of tyramine and HK853 (G) ^{1}H STD-NMR spectrum of tyramine and HK853.

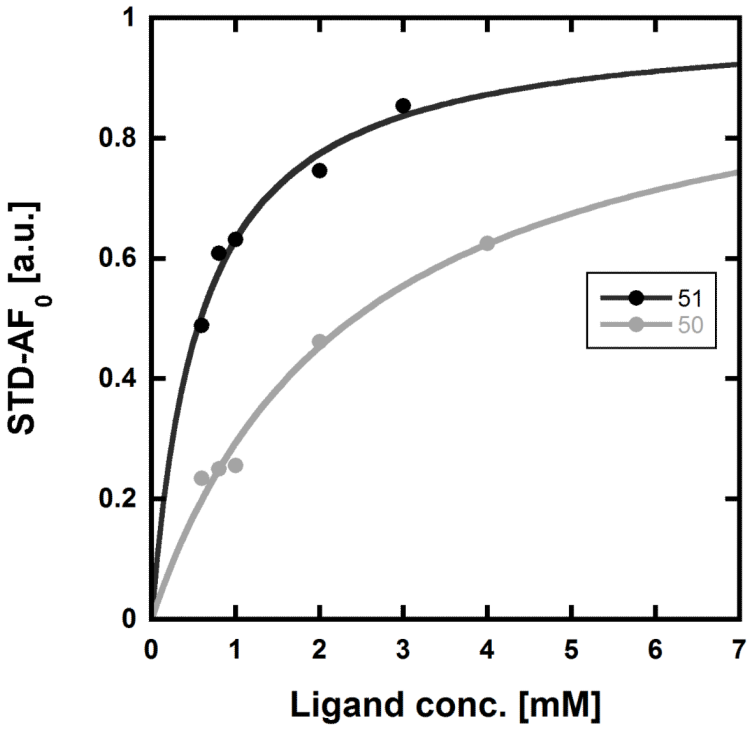

Fig. 8.

Determination of the K_d values of compounds **50** and **51** using STD-NMR. Using the initial growth rates approach[53] and mathematical fitting to a Langmuir isotherm, the K_d values of **50** and **51** were found to be 2.41 (± 0.25) mM and 0.58 (± 0.06) mM, respectively.

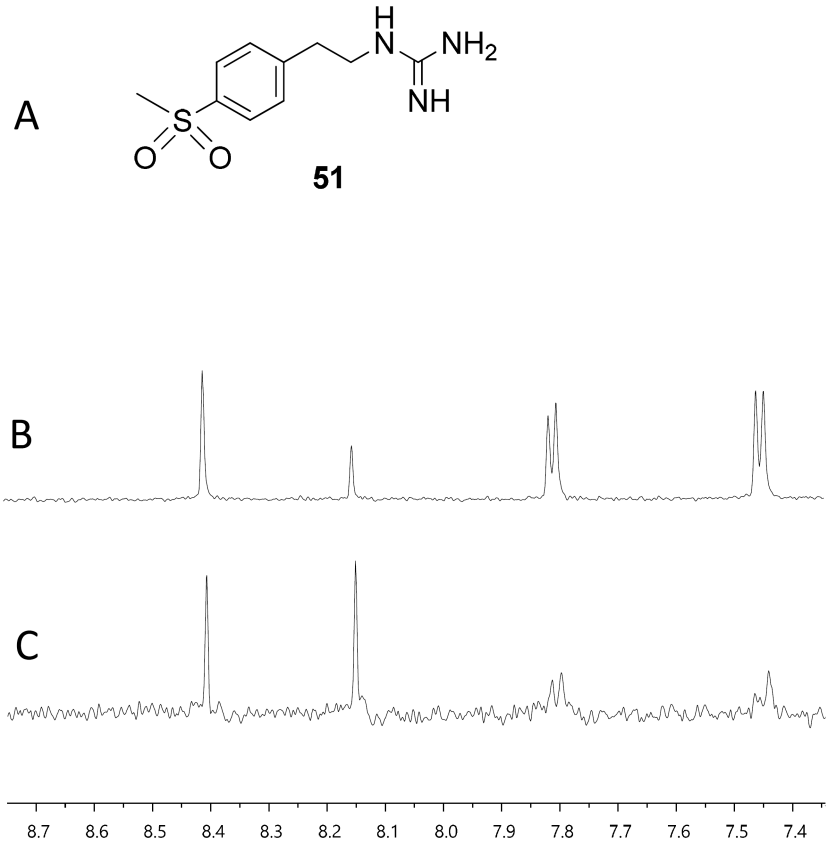

Fig. 9.

Assessment of binding using saturation transfer differential (STD) experiments (A) Compound **51** (B) ^{1}H spectrum of **51**, ADP and HK853 (C) ^{1}H STD-NMR spectrum of **51**, ADP and HK853.

Table 1

STD Factor values of compounds binding to HK853

Entry	Compound	f_{STD} [a]
1	Tyramine	16.6
2	ADP	73.3
3	**50**	28.4
4	**51**	32.8

[a]Aromatic peak resonances.